Modeling aqueous humor collection from the human eye

Konstantinos Kapnisis, Mark Van Doormaal, C. Ross Ethier *

Department of Bioengineering, Imperial College London, London SW7 2AZ, United Kingdom

ARTICLE INFO

ABSTRACT

Glaucoma is a common cause of blindness. Studies of this disease can involve collection of aqueous humor (AH) fluid from eyes of patients undergoing surgery, which involves aspirating a small fluid volume from the anterior region of the eye through a fine-bore needle. Unfortunately, the composition of the AH is spatially non-uniform in the eye, and thus the composition of the aspirated fluid is uncertain. Our goal was to numerically simulate the AH aspiration process to determine where the aspirated fluid was being collected from and thus gain insight into the composition of the collected fluid.

A 3D computational model of the anterior region of the human eye was created and the Navier–Stokes equations were numerically solved during the aspiration process for a set of typical (baseline) conditions: 40 µl aspirated volume and needle placement in the central anterior chamber. We also ran variations of this baseline simulation.

The main finding was that the aspirated fluid comes from a very localized region around the needle tip, so that for typical conditions, almost no aspirated fluid is withdrawn from the angle region of the anterior chamber. This is important because the AH in this angle region is protein-rich and directly interacts with the tissues that control fluid drainage from the eye. Recommendations for standardizing aspiration conditions are given.

© 2009 Elsevier Ltd. All rights reserved.

1. Introduction

Approximately 65 million people worldwide suffer from glaucoma, making it the second most common cause of blindness in western countries (Quigley, 1996). In most cases of glaucoma, the pressure within the eye is elevated, due to a partial obstruction of the outflow tissues responsible for drainage of aqueous humor (AH) fluid from the eye (Ethier et al., 2004) (see Fig. 1 for anatomy and terminology). The cause of this obstruction is not known and is a major topic of research.

There is evidence that AH composition changes in glaucoma (Tripathi et al., 1994; Picht et al., 2001; Liton et al., 2005) and that AH substantially affects cellular physiology in the outflow tissues (Fautsch et al., 2005). This has motivated investigators to collect and analyze AH, e.g. (Nolan et al., 2007). Collection is accomplished by insertion of a needle into the anterior chamber of the eye and aspiration of a small volume of AH from eyes of patients undergoing surgery for glaucoma or for cataract (as a control group). However, the composition of the AH is non-uniform in vivo, with the protein content of the fluid in the angle of the anterior chamber (Fig. 1) being markedly enriched (Freddo et al., 1990; Barsotti et al., 1992; Bert et al., 2006). Thus, AH aspiration

from the central anterior chamber, which is the collection location used in some studies, may collect fluid that is not representative of the AH that is interacting with the outflow tissues.

Our goal was to understand flow patterns in the eye during a typical AH aspiration so as to determine whether the collected fluid included the protein-rich AH from the angle of the anterior chamber. To do so, we used finite element modeling.

2. Materials and methods

Because of patient-to-patient and surgeon-to-surgeon differences, the aspiration process is not perfectly repeatable. We thus created a baseline model of the aspiration process based on typical values, and then carried out additional simulations by varying key parameters in the baseline model.

Baseline model: a geometric model of the anterior and posterior eye segments was created from measurements (Table 1) using ANSYS ICEM. Symmetry was assumed so that the computational domain consisted of only half of the geometry. The posterior cornea was approximated as a sphere of radius 7.1 mm, which, together with the measurements in Table 1, gives an anterior chamber volume of approximately 189 µL. This volume, and the other measures given in Table 1, agree well with clinical measurements. For example, in 624 eyes Fontana and Brubaker (1980) measured an anterior chamber volume of 199 ± 48 µL (mean $\pm$ standard deviation), a central depth of 3.0 ± 0.4 mm and a diameter of 12.8 ± 0.6 mm. Both anterior chamber volume and central depth decrease with age, and the values that we have chosen are most appropriate for individuals in the range 41–50 years.

AH was aspirated using a small syringe attached to a 30-gauge needle which entered the peripheral anterior chamber (AC) at the limbus, on a plane approximately parallel with the long axis of the elliptical lens. Based on

* Corresponding author. Tel.: +44 20 7594 9794; fax: +44 20 7594 9787.
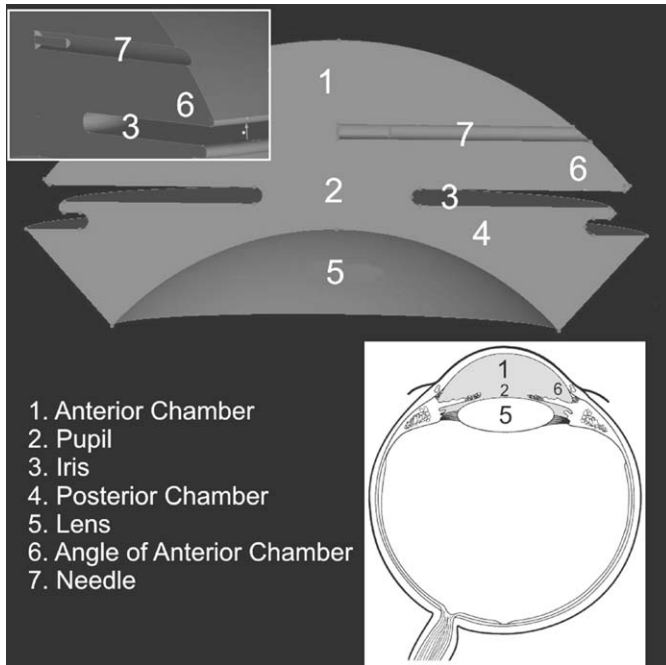E-mail address: r.ethier@imperial.ac.uk (C. Ross Ethier).

Fig. 1. Schematic view of eye (in cross-section at lower right, with modeled region colored gray) and model used for simulations. The inset at upper left shows a zoomed view of the edge of the model. The truncated length of the needle lumen can be observed. Note that not all elements are labeled in each portion of the figure. Aqueous humor in the angle of the anterior chamber (region 6) is known to be enriched in protein content.

Table 1
Assumed parameter values for an adult human eye.

Physical quantity	Typical value (mm)
Diameter of anterior chamber	11.8
Central depth of anterior chamber	3.15
Coronal radius of lens	4.50
Axial radius of lens	2.00
Iris thickness	0.34
Pupil diameter	3.00
Lens–Iris gap	0.50

Most values were directly measured from a cross-section of an eye (Krey and Bräuer, 1998); the lens–iris gap was assumed.

descriptions of the aspiration technique, we assumed that the entry point was 1.84 mm below the surface of the cornea. The needle penetrated the AC until its tip was approximately in the middle of the anterior chamber. AH was considered to have physical properties similar to saline at 37 °C (Beswick and McCulloch, 1956; Hoffert and Fromm, 1969; VanBuskirk and Grant, 1974), and was withdrawn at 8 µl/s from the AC, corresponding to a typical surgical aspiration of 40 µl of AH in 5 s. The corresponding Reynolds number based on mean needle lumen velocity and needle lumen diameter was Re = 105.2.

During the AH withdrawal process, the anterior chamber partially collapses. This was prohibitively complex to model, so we simplified the problem as follows: we kept the anterior chamber geometry the same throughout the withdrawal process by supplying extra fluid uniformly from the tissues bounding the anterior and posterior chambers so as to just balance the withdrawal rate. For typical aspiration volumes of 40 µl and anterior chamber volumes of 140–200 µl (Fontana and Brubaker, 1980; Wang et al., 2007), this is a reasonable first approximation, which we further investigate below. The fluid outlet in the computational model was the distal end of the needle lumen; we chose to model a lumen length of only 7.5 times the inner diameter of the lumen. This length was chosen because it was sufficiently long that the outflow boundary conditions applied at this location did not affect the flow near the needle tip.

The geometry was meshed using 10-noded tetrahedra, producing a mesh containing 962,689 elements and 1,259,201 nodes. We solved the steady, 3D Navier–Stokes equations on this mesh using an existing, well-validated finite element package (Ethier et al., 1998, 1999). Numerical convergence was verified and mesh independence was confirmed on a sequence of 3 progressively refined meshes (Kapnisis, 2008).

Variations of the baseline simulation: seven additional simulations were carried out, each changing a different aspect of the baseline model, to investigate their effects on AH aspiration patterns.

Simulations were first carried out to investigate the effects of aspiration speed, in which we doubled and halved the baseline aspiration speed while keeping the total aspirated volume the same, corresponding to needle Reynolds numbers of 52.6 and 210.4. A third simulation investigated the effects of posterior chamber collapse by infusing fluid only through the bounding tissues of the anterior chamber. The fourth simulation studied the effects of partial anterior chamber collapse during the aspiration process. After the aspiration of 40 µl of AH, the volume of the AC is reduced in reality. Hence, we created a new CAD model of the anterior segment of the eye in which the anterior–posterior dimensions of the AC were diminished so that the volume of the AC was reduced by 40 µl. In the fifth simulation we investigated the effect of a different needle position by creating a new model in which the needle penetrated further into the AC so that its tip was located 75% of the way across the chamber. In the sixth simulation we more accurately modeled the effects of needle tip geometry by including a needle beveled at 45°, rather than a blunt end. This was carried out for the case of no posterior chamber collapse. Finally, in the seventh simulation, we decreased the lens–iris gap to a more physiologic value of 0.05 mm while again having no posterior chamber collapse.

3. Results

Under baseline conditions, the aspirated AH came almost exclusively from the central AC, with some fluid withdrawn from the posterior chamber near the pupillary opening. Essentially no
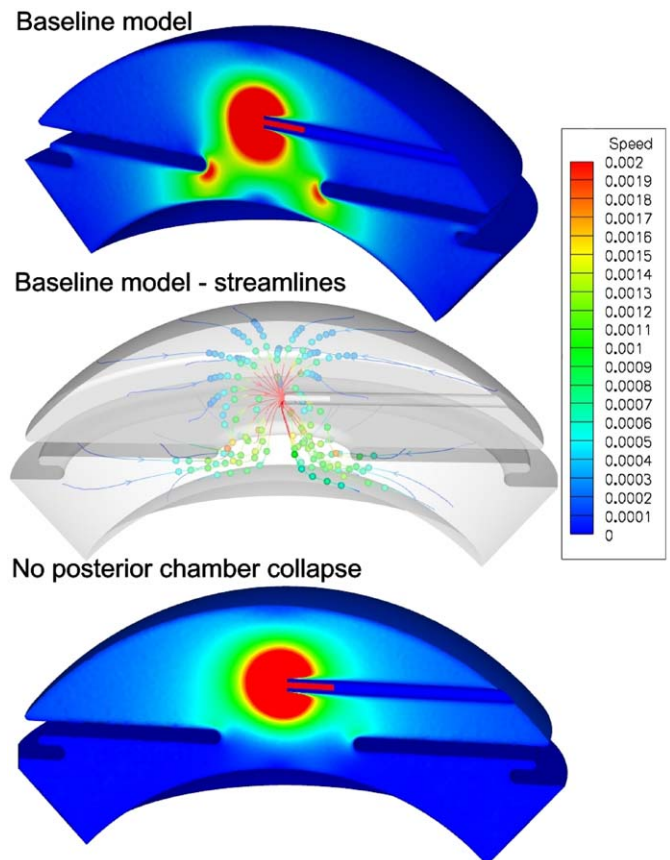

Fig. 2. Contours of fluid speed on the model symmetry plane (top and bottom panels) and fluid streamlines (middle panel). The upper two panels are for the baseline case, while the lower panel is for the case where no fluid enters the domain from the posterior chamber walls (see text). In the streamline plot, balls are placed at 1 s intervals, i.e. the balls closest to the needle tip indicate fluid that reaches the needle tip 1 s after the start of aspiration, the second set of balls indicates fluid that reaches the needle in 2 s, etc. The balls furthest from the needle tip therefore delimit the fluid that is collected during the 5 s aspiration process. Speeds have been made dimensionless with respect to the mean fluid speed in the needle.